Extremely Elastic Wearable Carbon Nanotube Fiber Strain Sensor for Monitoring of Human Motion

Seongwoo Ryu,[†,‡,§] Phillip Lee,[†,§] Jeffrey B. Chou,[†] Ruize Xu,[†] Rong Zhao,[‡] Anastasios John Hart,[†] and Sang-Gook Kim[*,†]

[†]Department of Mechanical Engineering, Massachusetts Institute of Technology (MIT), 77 Massachusetts Avenue, Cambridge, Massachusetts 02139, United States and [‡]Engineering Product Development, Singapore University of Technology and Design (SUTD), 20 Dover Drive, Singapore 138682, Singapore. [§]These authors contributed equally.

ABSTRACT The increasing demand for wearable electronic devices has made the development of highly elastic strain sensors that can monitor various physical parameters an essential factor for realizing next generation electronics. Here, we report an ultrahigh stretchable and wearable device fabricated from dry-spun carbon nanotube (CNT) fibers. Stretching the highly oriented CNT fibers grown on a flexible substrate (Ecoflex) induces a constant decrease in the conductive pathways and contact areas between nanotubes depending on the stretching distance; this enables CNT fibers to behave as highly sensitive strain sensors. Owing to its unique structure and mechanism, this device can be stretched by over 900% while retaining high sensitivity, responsiveness, and durability. Furthermore, the device with biaxially oriented CNT fiber arrays shows independent cross-sensitivity, which facilitates simultaneous measurement of strains along multiple axes. We demonstrated potential applications of the proposed device, such as strain gauge, single and multiaxial detecting motion sensors. These devices can be incorporated into various motion detecting systems where their applications are limited to their strain.

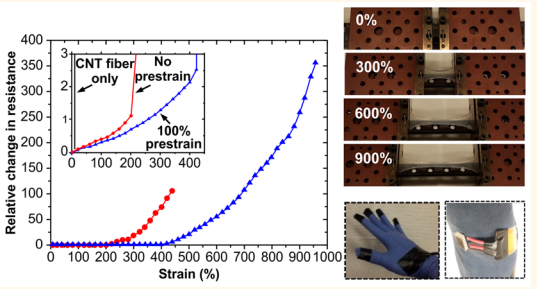

KEYWORDS: carbon nanotube · fiber · strain sensor · elastic electrode · wearable device

The demand for smart devices has risen exponentially in recent years. Flexibility and elasticity need to be essential features of the next generation of wearable electronics.[1−8] There are significant efforts underway to develop highly elastic strain sensors that can monitor physical activity, health-related parameters such as breathing, the healing of wounds, and other user-related variables.[9−11] Various attempts have been made to produce such highly elastic sensors. Nanoscale metal films,[12] metal films on flexible substrates,[13] and metal−polymer composite structures[14] have been investigated for use in such sensors; however, the semiconductor materials used in these devices are brittle and allow only small strains. Recent research on strain sensors has focused on the use of nanoscale carbon materials to circumvent the problems associated with brittle silicon materials.[15−19] Nanoscale carbon materials can be used as strain-sensing materials either individually[20,21] or as conductive fillers in soft polymers.[4,22] Among these materials, carbon nanotubes (CNTs), which have a quasi-one-dimensional structure, have attracted considerable attention. Because of their unique sp^2-bonded honeycomb lattice and one-dimensional structure, carbon nanotubes have superior mechanical and electrical properties.[23,24] The ability to form conductive networks of CNTs offers the possibility of fabricating highly elastic strain sensors[9,25] in which the one-dimensional structure of CNTs can be exploited for detecting large strains. However, such sensors would exhibit low repeatability under cyclic service conditions[26] and poor stability with respect to electrical resistance, owing to current breakdown.[27,28] In this paper, we describe a highly elastic strain sensor based on CNT fibers fabricated by the dry-spinning process, which can produce CNTs with a one-dimensional structure. Placing highly oriented CNT fiber arrays on

* Address correspondence to sangkim@mit.edu.

Received for review January 27, 2015 and accepted June 3, 2015.

Published online June 03, 2015
10.1021/acsnano.5b00599

an elastic substrate resulted in a uniform stress distribution over the entire device when it was stretched. The fabricated strain sensor exhibited a remarkably high tolerance to tensile strains (greater than 900%) along the CNT longitudinal axis, as well as high sensitivity, a fast response time, and high durability. Further, the axial elasticity of the sensor allowed it to simultaneously sense strains along multiple axes.

RESULTS AND DISCUSSIONS

Figure 1a illustrates the process for fabricating the CNT-fiber-based strain sensor. The CNT fibers were produced using the dry-spinning process, which can be used to create highly oriented CNT arrays.[29,30] The CNT fibers were spun directly from vertically aligned CNT arrays. These vertically aligned CNT arrays were grown by chemical vapor deposition using an Fe catalyst immobilized on a Si substrate. Figure 1b shows a photograph and SEM images of 250-μm- high CNT arrays interacting with neighboring CNTs. Owing to these van der Waals interactions, continuous fibers could be spun directly from the vertically aligned arrays. The density of the CNT fibers was calculated to be 0.298 g/cm^3 in the case of triple-walled CNTs (Supporting Information Figure S1). The aligned fibers were attached directly to an elastic substrate called Ecoflex (Figure 1c). Ecoflex is a platinum-catalyzed, highly elastic silicone material that can withstand strains greater than 900%. Dry-spun CNT fibers alone cannot tolerate strains greater than approximately 8% because of necking and stress concentration around the defects in the fibers.[20] However, using a flexible substrate for support ensures that the strain is distributed uniformly across the fibers, reducing necking and stress concentration. As a result, CNT fibers on an elastic substrate can be stretched to the strain limit of the substrate without the CNT fibers breaking. It can be observed from Figure 1c that the CNT-fiber strain sensor could be stretched to a strain of 900%.

Figure 1d shows the strain *versus* the relative change in the resistance, $(R/R_0) - 1$, where R_0 is the initial resistance of the strain sensor and R is its resistance when stretched; the values corresponding to drawn CNT fibers (black), CNT fibers on Ecoflex (red), and CNT fibers on prestrained Ecoflex (blue) are shown. In contrast to the case of the drawn CNT fibers (initial conductivity of 8.12 $\Omega\cdot$cm), which failed at a strain of approximately 8%, a monotonic linear increase in resistance was observed—along two different gauge factors (GF)—in the case of the Ecoflex-supported CNT-fiber-based strain sensor (initial conductivity of 0.917 k$\Omega\cdot$cm). The GF is a measure of the sensitivity of the strain sensor and is defined as follows: GF = (dR/R)/(dL/L), where R is the resistance and L is the length of the strain sensor. For strains of 0% to 200%, the relative change in the resistance of the Ecoflex-supported CNT-fiber-based strain sensor increased by a factor of 1.13 (GF: 0.56). From strains of 200% to 440%, at which point the sensor failed, the relative change in the resistance increased by a factor of 106 (GF: 47). The value of the gauge factor for strains greater than 200% was approximately 100 times greater than that for strains lower than 200%. This difference in the gauge factor reveals that there are two different mechanisms affecting the resistance under deformation, as shown in Figure 1e. The irreversible sliding of the CNTs causes pull out and subsequent buckling (Supporting Information Figure S2), resulting in local disconnections between the CNT bundles. At low strains, a regime we named the "sliding phase," local disconnections were not observed; however, for strains greater than 200%, a regime we named the "disconnecting phase," local disconnections occurred between the CNT bundles.

Introducing a preliminary strain in the elastic substrate is a known approach for improving the elasticity of films transferred onto the substrate.[31,32] This approach decreases the intrinsic strain on the structures in the device and improves the elastic performance of the device.[33,34] CNT fibers were attached to the Ecoflex substrate while it was subjected to initial strains of up to 100%. Releasing the tension in the Ecoflex substrate allowed it to contract to its initial length, causing an increase in the elasticity of the CNT arrays. The CNT devices fabricated using prestrained substrates (initial conductivity of 0.389 k$\Omega\cdot$cm) were able to function at strains of up to 960% (Figure 1d, blue line). For strains of 0% to 400% and 400% to 960%, the relative changes in the resistance increased from 0 to 2.14 (GF: 0.54) and 2.14 to 358 (GF: 64), respectively. Compared to the unstretched-substrate device (red line), the strain range of the sliding-phase device and that of the disconnecting-phase device was more than twice as large. It can be observed from the SEM images in Figure 1f that local disconnections appeared in the structure for strains greater than 400% (Supporting Information Figure S3). A decrease in the intrinsic strain produced a more uniform strain in the CNT fibers, which prevented local disconnections in the fibers and subsequently increased the elasticity of the device.

The schematic in Figure 1g explains the mechanism underlying the change in the resistance for the two ranges of stretching. In contrast to the electrical resistance of individual CNTs, the contact resistance between CNTs is so large that the resistance of the device depends on the effective contact area between the individual CNTs. According to the tunneling model, the initial resistance of a CNT fiber (R) can be determined using the following expression: $R = (8\pi hL/3A^2XdN)e^{Xd}$, where $X = 4\pi(2m\Phi)^{1/2}/h$, d is the tunneling distance, h is Planck's constant, L is the number of CNTs forming a single conducting path, N is the number of conducting paths, A^2 is the effective cross-sectional area, and Φ is the height of the potential barrier between adjacent

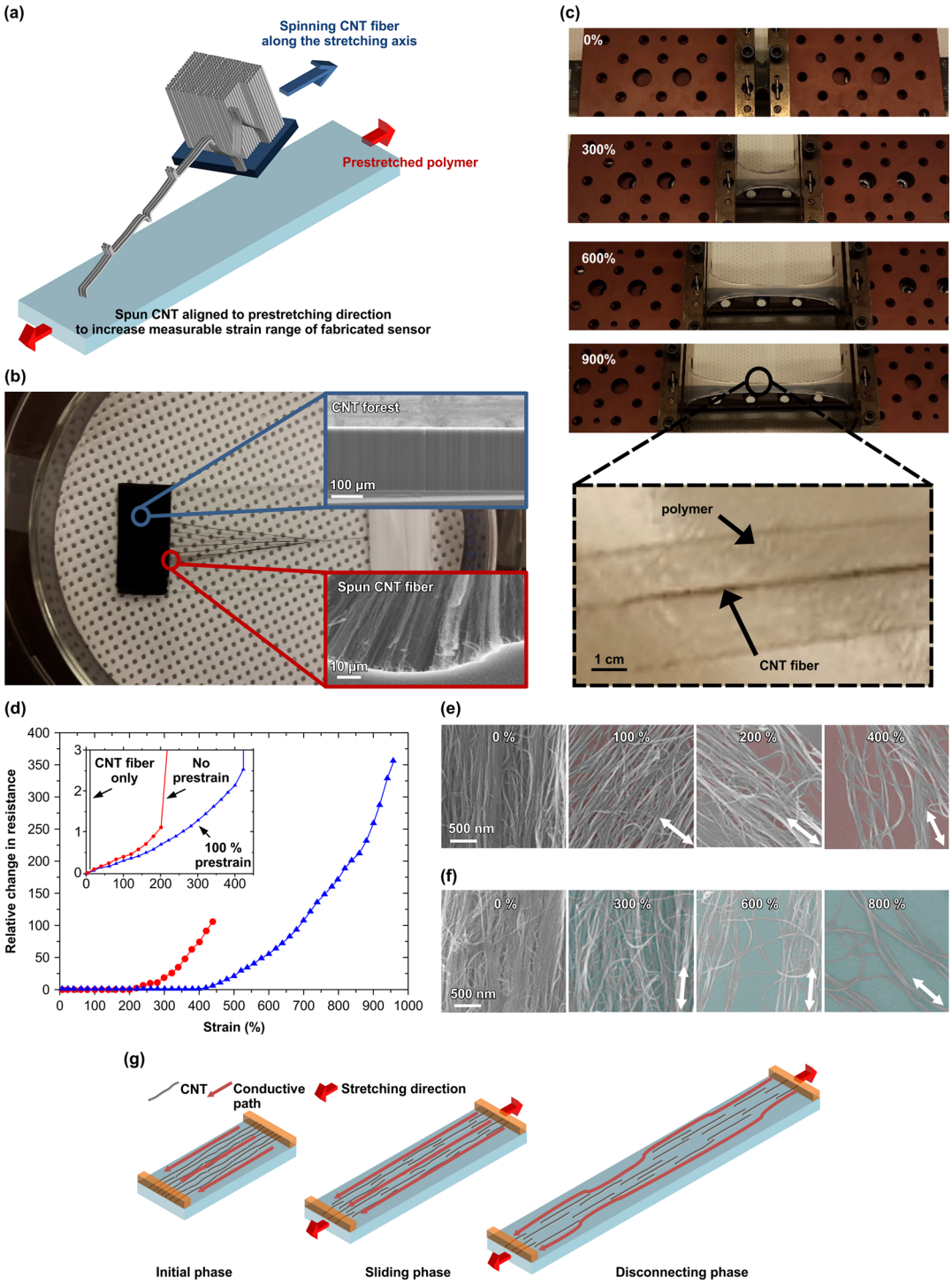

Figure 1. Extremely elastic CNT-fiber-based strain sensor. (a) Illustration of the fabrication process. The dry-spun CNT fibers attach directly to the elastic Ecoflex substrate. (b) Photograph of the dry-spinning process and SEM images of the fibers: vertically aligned CNT arrays obtained using the dry-spinning process (upper inset) and dry-spun CNT fibers (lower inset). (c) Photographs of the strain sensor being stretched parallel to the direction of orientation of the CNT fibers. The structure of the CNT fibers remains intact up to a strain of 900%. (d) Relative change in resistance *versus* strain for unsupported CNT fibers (black), CNT fibers on an unstrained Ecoflex substrate (red), and CNT fibers on an Ecoflex substrate prestrained by 100% (blue); the strain ranged from 0% to 450% strain (inset). (e) SEM images of CNT fibers on an Ecoflex substrate for various strains. (f) SEM images of CNT fibers on an Ecoflex substrate prestrained by 100% for various strains. The arrows indicate the direction of the strain. (g) Schematic showing the morphology of a CNT fiber under strain.

CNTs.[35] In the initial sliding phase, the increase in the resistance is caused by a decrease in the contact area (*i.e.*, the effective cross-sectional area, A^2) between the sliding CNTs. Although the degree of contact between the wavy CNTs is low, the use of the elastic Ecoflex substrate decreases the effective cross-sectional area

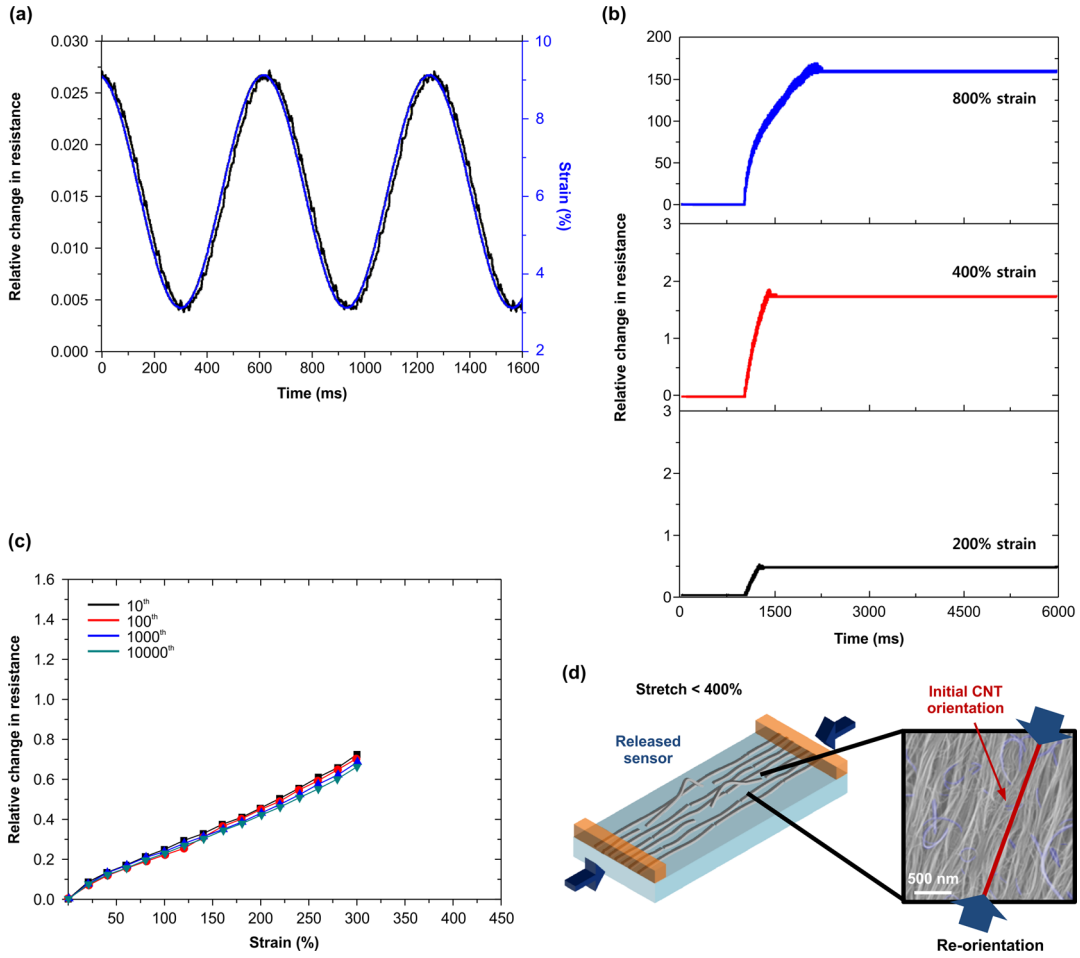

Figure 2. Sensitivity, stability, and durability of the CNT-fibers-based strain sensor (substrate prestrained by 100%). (a) Relative change in resistance (black) *versus* time for cycling at 1.5 Hz and strains between 3% and 9% (blue). (b) Relative change in resistance *versus* time for increases in the strain from 0% to 200% (black), 400% (red), and 800% (blue). Relative change in resistance *versus* strain for 10 (black), 1000 (red), 1000 (blue), and 10000 cycles (green) for increases in the strain from 0% to (c) 300% and (d) illustration and SEM image of CNT fibers after 10000 cycles.

between the CNTs in proportion to the applied strain. When the device is stretched beyond the sliding limit, the CNTs begin to disconnect. Because of the stress concentration and variations in the frictional force, a few CNTs get disconnected, while the rest of the CNTs remain in the sliding phase. The distances between the disconnected CNT bundles increase, decreasing the number of conductive paths (N) and increasing the number of CNTs forming a conductive path (L). Consequently, in the disconnecting phase, the effects of sliding and the disconnecting of the CNTs combine, resulting in an increase in the GF value. The microstructure of the synthesized CNTs (thickness, number of walls, and chirality, among others) as well as the dimensions of the CNT fibers (diameter, density, and number of defect sites) influence the sensitivity and transition phase of the sensor. Longer CNTs may increase the transition charge at the higher strain. Further, the GF will be affected by the density and alignment of the CNT fibers, as these parameters determine the contact area and the number of contacts. Dry spinning allows for the synthesis of highly oriented CNT array structures; however, it requires that there be optimized interactions between the CNTs. The CNTs used in the present study were limited in their microstructural properties (thickness, length, and number of walls, among others). These issues will be examined in future studies.

The fabricated devices exhibited fast responses, good stability, and high durability. The responses of the strain sensors were measured by applying a cyclic load with a position-recorded actuator (Instron 8848); the relative change in the resistance with respect to time is shown in Figure 2a. To avoid a delay between the detectors, the electrical signal was received using the same detector. The delay in the strain sensor, which was determined from the sinusoidal signal, was 10 ms when the strain was increasing and 12 ms when the strain was decreasing. These results indicate that the CNT arrays could respond almost immediately to external strains. The strain sensor was stretched and maintained at strains of 200%, 400%, and 800% (Figure 2b); the stretched sensor showed overshoots of only 1.0%, 1.2%, and 2.2%, respectively; the resistance

remained stable and the recovery time was 12 ms. The sensor was subjected to numerous loading−unloading cycles, and exhibited stable properties for up to 10 000 cycles. From strains of 0% to 300% in the sliding phase, the sensitivity of the strain sensor stabilized with a GF of 0.26 at the 10th cycle and remained at 93% (0.24) after 10 000 cycles (Figure 2c). Figure 2d shows SEM images obtained after 10 000 cycles during the sliding phase; it can be observed that the alignment of most of the CNT bundles was retained even after the loading/unloading cycles. The initial orientation of the microscale structure was maintained. The GF decreased further in the disconnecting phase (42%) after 10 000 cycles (Supporting Information Figure S4). A corresponding decrease in the sensitivity occurred owing to structural deformation (Supporting Information Figure S5). This decrease in the sensitivity is primarily due to an increase in the initial resistance (Supporting Information Figure S6). Although the decrease in the sensitivity in the disconnecting phase is greater than that in the sliding phase, the initial conductivity of this device remained at 26.891 kΩ·cm, while the GF value remained at 22 after 10 000 cycles. Thus, the device has high potential as a sensor at extremely high strains. In future studies, we aim to minimize the degradation in the cyclic performance of the sensor by preventing the deformation of the CNT arrays. This extremely elastic strain sensor may be used as an ordinary strain gauge (see Supporting Information Figure S7) or in applications and devices requiring high elasticity such as artificial skin and wearable electronic devices.[25,36] Figure 3 illustrates some of the possible applications. By attaching these sensors to a pair of tights using Ecoflex glue, we could measure the complex motion of human joints. The motions of the knee and hamstring could be measured simultaneously during the basic act of jumping (Figure 3a). In the initial squatting position, the knee was flexed, causing the knee sensor to stretch and its relative resistance to increase, and the hamstring muscles contracted, causing the hamstring sensor to contract and its resistance to decrease. When the wearer jumped, with the jump lasting from the 400 ms point to the 800 ms point, the knee extended, causing the knee sensor to contract and its relative resistance to decrease, while the hamstring muscle lengthened, causing the hamstring sensor to stretch and its relative resistance to increase. When the wearer's feet touched the ground, the knee joint flexed and the hamstring muscles contracted for a short period (from 800 to 1200 ms) to absorb the impact, and the wearer returned to the initial squatting position. Figure 3b demonstrates the potential of the wearable strain sensor for detecting motion as well as the movement of the fingers. We fabricated elastic motion sensors by attaching CNT arrays to a conventional latex glove. The latex glove was first coated with a thin layer of Ecoflex. The CNT fibers were dry spun and attached directly to the Ecoflex substrate prestrained by 100%. The ends of the fibers were connected to electrodes composed of a silver paste and Ecoflex. To prevent the CNT fibers from separating from the electrodes during stretching, the junctions between the CNT fibers and the electrodes were covered with solid tape. The complex motion of the fingers was measured using five independent CNT fibers, each attached to a different finger. The delays and the strains associated with the finger movements were monitored using both the strain sensors (Figure 3b) and images (Figure 3b upper photo) obtained during the experiment. We could successfully monitor the grasping and releasing motions of the hand over a period of 1.5 s. The grasping motion, which involved four fingers, began after 0.411 s, while the thumb remained in the relaxed position. The thumb became involved in the grasping motion 0.170 s after the fingers had started moving. The releasing motion was initiated instantly in all the fingers in 0.158 s. The strain from the fingers was determined by comparing the results of the measurements of the respective CNT-fiber-based strain sensors in the same cycle. The maximum strain measured during the movement of the individual joints was estimated to be 55%. However, the movement of multiple joints requires sensors that can detect larger strains, as fingers have multiple joints and exhibit different strains. Figure 3b shows the relative change in resistance and the estimated strains as measured for the fingers. The thumb, which has two joints, exhibited a strain of 120%, whereas the other fingers, which have three joints, exhibited strains greater than 200% (index, 241%; middle, 297%; ring, 275%; and little, 218%).

A biaxial strain sensor can measure strains in two dimensions instead of only one.[37,38] Highly elastic strain sensors are useful for the simultaneous measurement of strains along multiple axes and can be employed as wearable sensors. Figure 3c shows the process for fabricating a biaxial CNT-fiber-based strain sensor. The CNT fibers were directly dry spun and bonded to the Ecoflex substrate through van der Waals interactions. This process was repeated after rotating the Ecoflex substrate by 90°. As shown in the SEM image in Figure 3d, the CNT arrays were oriented biaxially at an angle of 90°. When stacked in multiple layers, the CNT fibers in these arrays could respond nearly independently to strains along their alignment directions. We observed a small degree of cross-sensitivity between the two axes. Figure 3e shows the relative change in the resistance along the *x*-axis for a strain applied along the *x*-axis in the case of the array fixed along the *y*-axis. For a strain of 200% along the *x*-axis, there was a slight increase in the resistance along the *y*-axis (0.019 when there was no *y*-axis strain and 0.022 for a *y*-axis strain of 200%); however, the *x*- and *y*-axis CNT fibers responded independently. This feature is essential for monitoring biaxial movements

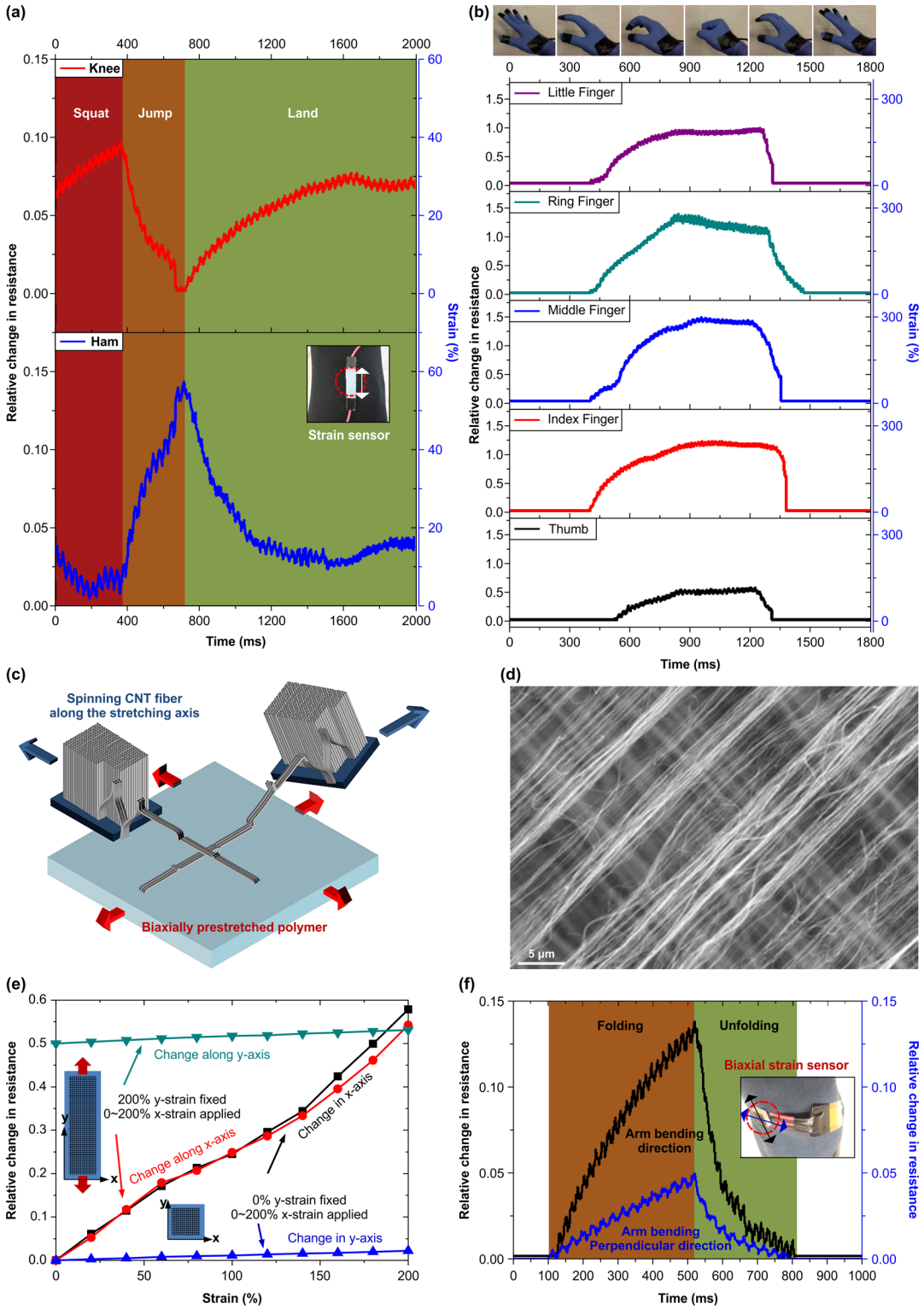

Figure 3. Wearable, extremely elastic CNT-fibers-based strain sensor (substrate prestrained by 100%). (a) Relative change in resistance (and estimated strain) *versus* time while jumping for strain sensors placed over a knee joint and hamstring muscles. (b) Photograph of a wearable strain sensor glove and relative changes in resistance (and estimated strain) *versus* time for grasping motion. (c) Illustration of the process for fabricating a biaxial strain sensor. (d) SEM image of biaxial strain sensor. (e) Relative changes in resistance *versus* strain for a biaxial CNT-fiber strain sensor: *x*-axis resistance with variable *x*-axis strain and *y*-axis at constant 0% strain (black), *y*-axis resistance with variable *x*-axis strain and *y*-axis at a constant 0% strain (blue), *y*-axis resistance with variable *x*-axis strain and *y*-axis at a constant 200% strain (red), and *y*-axis resistance with variable *x*-axis strain and *y*-axis at a constant 200% strain (blue). (f) Relative changes in resistance *versus* time for a biaxial strain sensor placed over an elbow, with the *x*-axis parallel to the arm (black) and the *y*-axis parallel to joint's axis of rotation (blue).

resulting in deformations in multiple axes. Figure 3f shows a biaxial strain sensor placed over an elbow. The strain sensor was placed with the *y*-axis parallel to the axis of rotation of the elbow joint and the *x*-axis parallel to the long axis of the arm (*i.e.*, the arm bones). The arm was initially extended. The elbow was then flexed and extended rapidly. Strains in both the *x*-axis and the *y*-axis began at 0.105 s, and the elbow returned to its initial position at 0.811 s. The maximum measured values of the strain were 48% along the *x*-axis and 15% along the *y*-axis. These results demonstrate that a CNT-fiber-based strain sensor has great potential for monitoring both the movements of the multiple joints of fingers and the biaxial movements of complex joints. In this study, we only tested the fabricated CNT-fiber-based strain sensors in a few configurations. However, it should be possible to align the CNT fibers in other directions as well in order to sense movements along multiple axes.

CONCLUSION

To conclude, in this study, we developed an extremely elastic strain sensor using highly oriented CNT fibers fabricated by dry spinning. As this device was fabricated on a flexible substrate, it could measure strains greater than 900% with high sensitivity and exhibited a fast response and good durability. To the best of our knowledge, no previously reported CNT-based sensors have exhibited this degree of elasticity and such high sensitivity. Such sensors should find wide use in applications in which large strains are involved, including in soft robotics. Further, highly elastic strain gauges have enormous potential for use in a variety of systems. These devices could be adapted for common strain gauge applications, the detection of animal and human motion, and many other applications requiring embedded and wearable devices.

METHODS

Synthesis of Vertically Aligned CNT Arrays. Vertically aligned CNT arrays were synthesized using a chemical vapor deposition (CVD) process (Sabre Tube Desktop Thermal Processing System). An Al (10 nm)/Fe (1.7 nm) catalyst layer was deposited on a Si wafer through thermal evaporation (Atech System). Argon (Ar) and hydrogen (H_2) were used as the carrier gases, and ethylene (C_2H_4) gas was used as the carbon source. To synthesize the vertically aligned CNT arrays, the temperature was raised to 750 °C for 10 min, and Ar was allowed to flow at 2000 sccm. Subsequently, 60 sccm of H_2 was added to the flow for 5 min. Finally, 1000 sccm of C_2H_4 gas and 1 sccm of O_2 were introduced to the flow for 10 min.

Fabrication of CNT-Fiber-Based Strain Sensor. To produce the elastic substrate, equal volumes of Ecoflex (Ecoflex Supersoft 0050, Smooth-On, Inc.) Part A and Part B were mixed and placed in a vacuum chamber to remove any air bubbles. The mixture was then cured at room temperature for 7 days. The cured Ecoflex was cut into rectangular strips. To produce the prestrained substrate, the cured Ecoflex stripes were clamped at both ends and stretched at a strain of 100%. To produce the epoxy bar strain sensor, an epoxy bar was coated with uncured Ecoflex. To produce the leg motion sensor, the cured Ecoflex substrate was attached to a fabric garment using Ecoflex glue. To fabricate the finger motion sensor, a latex glove was coated with uncured Ecoflex. The CNT fibers were dry spun directly and became attached to the surfaces of the Ecoflex substrates prestrained by 100% owing to van der Waals interactions. The attached CNT fibers were coated with a thin film of Ecoflex during the curing process to prevent the separation of the fibers from the substrate. To measure the relative change in the resistance with strain, conductive electrodes were attached to the strain sensors with clamps. To measure the movement of the epoxy bar, the knee joint, the hamstring muscles, and the fingers, the electrodes of the strain sensors were connected to wires using a silver paste and covered with rigid tape. To fabricate the biaxial strain sensor, the process used to produce the single-axis sensor was repeated after rotating the substrate by 90°, and the resulting array was covered with a thin film of Ecoflex. To measure the elbow movements, the biaxial strain sensor was attached to a fabric garment using Ecoflex glue

Characterization. Scanning electron microscopy (XL30SFEG, Philips) was used to observe the microstructure of the CNT arrays during stretching and after cycle testing. A NI USB-6210 data acquisition (DAQ) board was used to measure the relative change in the resistance as the sensors were stretched. The sensors were connected across a DC voltage source (at constant voltage), and the voltage drop across the strain sensor (which acted as a resistor) was measured by the DAQ board; the results were observed on a computer using LabVIEW. A microforce testing system (Instron 8848, Instron) was used to apply the cyclic strains, constant stresses, strains, and displacements to the strain sensors. Transmission electron microscopy (JEM-3010, JEOL) was used to observe the microstructure of the CNTs. The weight of an individual CNT fiber 3 m in length was measured; the fiber weighed 1.2 mg. Further, the calculated volume of the fiber was 4.014 mm^3, and the density of the CNT fiber was 0.298 g/cm^3. The elasticity of the strain sensor was calculated from the GF value measured over one cycle.

Conflict of Interest: The authors declare no competing financial interest.

Supporting Information Available: TEM image of vertically aligned CNT arrays; SEM images of CNT fibers on prestrained and nonprestrained Ecoflex substrates under different strains; illustration and SEM images of CNT fibers after 10 000 cycles; and graphs depicting relative change in resistance *versus* strain, initial strain sensor resistance *versus* number of cycles, and relative change in resistance *versus* time of the strain sensor. The Supporting Information is available free of charge on the ACS Publications website at DOI: 10.1021/acsnano.5b00599.

Acknowledgment. This work was supported by the SUTD-MIT Postdoctoral Program.

REFERENCES AND NOTES

1. Rogers, J. A.; Someya, T.; Huang, Y. Materials and Mechanics for Stretchable Electronics. *Science* **2010**, *327*, 1603–1607.
2. Takei, K.; Takahashi, T.; Ho, J. C.; Ko, H.; Gillies, A. G.; Leu, P. W.; Fearing, R. S.; Javey, A. Nanowire Active-Matrix Circuitry for Low-Voltage Macroscale Artificial Skin. *Nat. Mater.* **2010**, *9*, 821–826.
3. Argun, A. A.; Cirpan, A.; Reynolds, J. R. The First Truly All-Polymer Electrochromic Devices. *Adv. Mater.* **2003**, *15*, 1338–1341.
4. Sekitani, T.; Noguchi, Y.; Hata, K.; Fukushima, T.; Aida, T.; Someya, T. A Rubberlike Stretchable Active Matrix Using Elastic Conductors. *Science* **2008**, *321*, 1468–1472.
5. Ahn, B. Y.; Duoss, E. B.; Motala, M. J.; Guo, X.; Park, S.-I.; Xiong, Y.; Yoon, J.; Nuzzo, R. G.; Rogers, J. A.; Lewis, J. A. Omnidirectional Printing of Flexible, Stretchable, and

Spanning Silver Microelectrodes. *Science* **2009**, *323*, 1590–1593.
6. Kim, Y.; Zhu, J.; Yeom, B.; Di Prima, M.; Su, X.; Kim, J.-G.; Yoo, S. J.; Uher, C.; Kotov, N. A. Stretchable Nanoparticle Conductors with Self-Organized Conductive Pathways. *Nature* **2013**, *500*, 59–63.
7. Lipomi, D. J.; Tee, B. C. K.; Vosgueritchian, M.; Bao, Z. Stretchable Organic Solar Cells. *Adv. Mater.* **2011**, *23*, 1771–1775.
8. Lee, J.; Lee, P.; Lee, H. B.; Hong, S.; Lee, I.; Yeo, J.; Lee, S. S.; Kim, T. S.; Lee, D.; Ko, S. H. Room-Temperature Nanosoldering of a Very Long Metal Nanowire Network by Conducting-Polymer-Assisted Joining for a Flexible Touch-Panel Application. *Adv. Funct. Mater.* **2013**, *23*, 4171–4176.
9. Yamada, T.; Hayamizu, Y.; Yamamoto, Y.; Yomogida, Y.; Izadi-Najafabadi, A.; Futaba, D. N.; Hata, K. A Stretchable Carbon Nanotube Strain Sensor for Human-Motion Detection. *Nat. Nanotechnol.* **2011**, *6*, 296–301.
10. Paradiso, R.; Loriga, G.; Taccini, N. A Wearable Health Care System Based on Knitted Integrated Sensors. *IEEE Trans. Inf. Technol. Biomed.* **2005**, *9*, 337–344.
11. Pang, C.; Lee, G.-Y.; Kim, T.-I.; Kim, S. M.; Kim, H. N.; Ahn, S.-H.; Suh, K.-Y. A Flexible and Highly Sensitive Strain-Gauge Sensor Using Reversible Interlocking of Nanofibres. *Nat. Mater.* **2012**, *11*, 795–801.
12. Khang, D.-Y.; Jiang, H.; Huang, Y.; Rogers, J. A. A Stretchable Form of Single-Crystal Silicon for High-Performance Electronics on Rubber Substrates. *Science* **2006**, *311*, 208–212.
13. Lacour, S. P.; Jones, J.; Wagner, S.; Li, T.; Suo, Z. Stretchable Interconnects for Elastic Electronic Surfaces. *Proc. IEEE* **2005**, *93*, 1459–1467.
14. Mattmann, C.; Clemens, F.; Tröster, G. Sensor for Measuring Strain in Textile. *Sensors* **2008**, *8*, 3719–3732.
15. Grow, R. J.; Wang, Q.; Cao, J.; Wang, D.; Dai, H. Piezoresistance of Carbon Nanotubes on Deformable Thin-Film Membranes. *Appl. Phys. Lett.* **2005**, *86*, 093104.
16. Dharap, P.; Li, Z.; Nagarajaiah, S.; Barrera, E. Nanotube Film Based on Single-Wall Carbon Nanotubes for Strain Sensing. *Nanotechnology* **2004**, *15*, 379–382.
17. Wang, Y.; Yang, R.; Shi, Z.; Zhang, L.; Shi, D.; Wang, E.; Zhang, G. Super-Elastic Graphene Ripples for Flexible Strain Sensors. *ACS Nano* **2011**, *5*, 3645–3650.
18. Hempel, M.; Nezich, D.; Kong, J.; Hofmann, M. A Novel Class of Strain Gauges Based on Layered Percolative Films of 2D Materials. *Nano Lett.* **2012**, *12*, 5714–5718.
19. Kim, K. S.; Zhao, Y.; Jang, H.; Lee, S. Y.; Kim, J. M.; Kim, K. S.; Ahn, J.-H.; Kim, P.; Choi, J.-Y.; Hong, B. H. Large-Scale Pattern Growth of Graphene Films for Stretchable Transparent Electrodes. *Nature* **2009**, *457*, 706–710.
20. Zhao, H.; Zhang, Y.; Bradford, P. D.; Zhou, Q.; Jia, Q.; Yuan, F.-G.; Zhu, Y. Carbon Nanotube Yarn Strain Sensors. *Nanotechnology* **2010**, *21*, 305502.
21. Jin, C.; Lan, H.; Peng, L.; Suenaga, K.; Iijima, S. Deriving Carbon Atomic Chains from Graphene. *Phys. Rev. Lett.* **2009**, *102*, 205501–205504.
22. Yu, Z.; Niu, X.; Liu, Z.; Pei, Q. Intrinsically Stretchable Polymer Light-Emitting Devices Using Carbon Nanotube-Polymer Composite Electrodes. *Adv. Mater.* **2011**, *23*, 3989–3994.
23. Dalton, A. B.; Collins, S.; Munoz, E.; Razal, J. M.; Ebron, V. H.; Ferraris, J. P.; Coleman, J. N.; Kim, B. G.; Baughman, R. H. Super-Tough Carbon-Nanotube Fibres. *Nature* **2003**, *423*, 703.
24. Geng, H.-Z.; Kim, K. K.; Song, C.; Xuyen, N. T.; Kim, S. M.; Park, K. A.; Lee, D. S.; An, K. H.; Lee, Y. S.; Chang, Y. Doping and De-Doping of Carbon Nanotube Transparent Conducting Films by Dispersant and Chemical Treatment. *J. Mater. Chem.* **2008**, *18*, 1261–1266.
25. Lipomi, D. J.; Vosgueritchian, M.; Tee, B. C.; Hellstrom, S. L.; Lee, J. A.; Fox, C. H.; Bao, Z. Skin-Like Pressure and Strain Sensors Based on Transparent Elastic Films of Carbon Nanotubes. *Nat. Nanotechnol.* **2011**, *6*, 788–792.
26. Thostenson, E. T.; Chou, T.-W. Real-Time *In Situ* Sensing of Damage Evolution in Advanced Fiber Composites Using Carbon Nanotube Networks. *Nanotechnology* **2008**, *19*, 215713.
27. Loh, K. J.; Kim, J.; Lynch, J. P.; Kam, N. W. S.; Kotov, N. A. Multifunctional Layer-By-Layer Carbon Nanotube–Polyelectrolyte Thin Films for Strain and Corrosion Sensing. *Smart Mater. Struct.* **2007**, *16*, 429–438.
28. Kang, I.; Schulz, M. J.; Kim, J. H.; Shanov, V.; Shi, D. A Carbon Nanotube Strain Sensor for Structural Health Monitoring. *Smart Mater. Struct.* **2006**, *15*, 737–748.
29. Jiang, K.; Li, Q.; Fan, S. Nanotechnology: Spinning Continuous Carbon Nanotube Yarns. *Nature* **2002**, *419*, 801.
30. Zhang, M.; Atkinson, K. R.; Baughman, R. H. Multifunctional Carbon Nanotube Yarns by Downsizing an Ancient Technology. *Science* **2004**, *306*, 1358–1361.
31. Lacour, S. P.; Wagner, S.; Huang, Z.; Suo, Z. Stretchable Gold Conductors on Elastomeric Substrates. *Appl. Phys. Lett.* **2003**, *82*, 2404–2406.
32. Kim, D. H.; Rogers, J. A. Stretchable Electronics: Materials Strategies and Devices. *Adv. Mater.* **2008**, *20*, 4887–4892.
33. Yu, C.; Masarapu, C.; Rong, J.; Wei, B.; Jiang, H. Stretchable Supercapacitors Based on Buckled Single-Walled Carbon-Nanotube Macrofilms. *Adv. Mater.* **2009**, *21*, 4793–4797.
34. Lee, P.; Lee, J.; Lee, H.; Yeo, J.; Hong, S.; Nam, K. H.; Lee, D.; Lee, S. S.; Ko, S. H. Highly Stretchable and Highly Conductive Metal Electrode by Very Long Metal Nanowire Percolation Network. *Adv. Mater.* **2012**, *24*, 3326–3332.
35. Zhao, J.; Zhang, G.-Y.; Shi, D.-X. Review of Graphene-Based Strain Sensors. *Chin. Phys. B* **2013**, *22*, 057701.
36. Kim, D.-H.; Lu, N.; Ma, R.; Kim, Y.-S.; Kim, R.-H.; Wang, S.; Wu, J.; Won, S. M.; Tao, H.; Islam, A. Epidermal Electronics. *Science* **2011**, *333*, 838–843.
37. Kim, D.-H.; Ahn, J.-H.; Choi, W. M.; Kim, H.-S.; Kim, T.-H.; Song, J.; Huang, Y. Y.; Liu, Z.; Lu, C.; Rogers, J. A. Stretchable and Foldable Silicon Integrated Circuits. *Science* **2008**, *320*, 507–511.
38. Choi, W. M.; Song, J.; Khang, D.-Y.; Jiang, H.; Huang, Y. Y.; Rogers, J. A. Biaxially Stretchable "Wavy" Silicon Nanomembranes. *Nano Lett.* **2007**, *7*, 1655–1663.